Electron-impact-like feature in triple fragmentation of CO_2^{3+} under slow proton impact

Sumit Srivastav and Bhas Bapat*

Indian Institute of Science Education and Research Pune, Homi Bhabha Road, Pune 411008, India

(Received 2 November 2021; accepted 15 December 2021; published 3 January 2022)

We have studied the three-body breakup of CO_2^{3+} created by the impact of slow ($v < 1$ a.u.) protons on CO_2. Employing the coincidence momentum imaging technique, we have obtained the correlated momenta of the three fragments, $O^+ + C^+ + O^+$, and thence the kinetic energy release (KER) distribution. By examining the Dalitz plots for the three-body breakup, we separate the sequential and concerted breakup events and analyze the corresponding KER distributions. Based on the potential energy curves reported in the literature, we identify the possible transient states of CO_2^{3+} that lead to the different features in the KER distribution. We find that under H^+ impact, the KER distribution shows a low-energy feature, which is seen in the case of electron impact, but not under the impact of slow or fast highly charged ions. This feature is identified as arising via the low-lying $^2\Pi$ and $^4\Pi$ states of the transient molecular ion. We further note that slow protons, which are the simplest of projectiles, are able to excite the CO_2 molecule to a broad range of triply ionized transient states, spanning those accessed by the impact of slow highly charged ions and also those accessed by electron impact, but with varying probabilities.

DOI: 10.1103/PhysRevA.105.012801

I. INTRODUCTION

The investigation of the breakup dynamics of multiply ionized polyatomic molecules has attracted attention over the past decade because of its importance in many fields of physics as well as in radiation biology [1–6]. Obtaining detailed kinematics of the breakup of polyatomic molecular ions has been a challenge because of the many-body nature of the dissociation. However, the combination of momentum spectrometry and advanced electronics has made these studies feasible and efficient [7,8]. In recent times, the break-up dynamics of molecular ions of various triatomic molecules, created under the impact of different projectiles, have been studied extensively [6,9–14].

The CO_2 molecule has received great attention as a prototype system in understanding many-body breakup dynamics. Neumann *et al.* reported pioneering results on three-body breakup dynamics of CO_2^{3+} created under the impact of slow Ar^{8+} ions on CO_2 [6]. They studied the kinetic energy release (KER) distribution of the $CO_2^{3+} \rightarrow O^+ + C^+ + O^+$ break-up and successfully separated the sequential and concerted bond-breaking mechanisms. They concluded that the total energy deposited into the system is the key parameter that controls the breakup dynamics. Following this work, CO_2^{3+} has been one of the most studied molecular cations, and the results of several experiments on its three-body breakup, created under the action of a variety of highly charged ions (HCI) at slow velocity ($v < 1$ a.u.) [6], intermediate velocity ($v \approx 1$ a.u.) [15], and swift velocity ($v > 1$ a.u.) [16–19], electron-impact [20,21], synchrotron radiation [22,23], or femtosecond laser pulses [24–27], have been reported. A large number of these investigations were centered around the question of how the breakup dynamics of multiply ionized molecular ions are influenced by specific projectiles.

Electrons and protons are the simplest charged projectiles that can produce multiply ionized molecular ions in collisions over a wide range of impact velocities. However, there are very few studies on triple or higher degrees of ionization of molecules by these projectiles. There is no report, to the best of our knowledge, on the three-body breakup $CO_2^{3+} \rightarrow O^+ + C^+ + O^+$ under the impact of H^+ ion, which we have investigated at two impact velocities, 0.5 and 0.83 a.u. (i.e., 6 and 17 keV). The $v < 1$ a.u. regime for protons and HCI is interesting, because here one expects competition between capture and direct ionization processes. The former implies capture of one or more electrons by the projectile, while the latter refers to removal of target electrons with no change in the projectile charge state. Using the coincidence momentum imaging technique, the momentum vector of each fragment was obtained, and the KER distributions for the breakup were derived. The sequential and concerted breakup mechanisms were separated using the Dalitz plot, and the KER distributions corresponding to the two mechanisms were extracted. The KER distributions for the two impact velocities were found to differ in the shapes, but intriguingly these distributions show a low-energy feature seen only under electron impact, and they span the higher KER range reported in the literature for slow HCI impact.

II. EXPERIMENTAL DETAILS

The present experiment has been carried out at the electron beam ion source (EBIS) facility at IISER Pune [28]. The source is manufactured by Dreebit GmbH, Germany, and it is capable of delivering multiply charged ion beams

*bhas.bapat@iiserpune.ac.in

with energies in the range of a few tens of keV/q. Fragments resulting from the collision were analyzed using a multihit capable ion momentum spectrometer. Details of the momentum spectrometer and the experimental setup have been reported earlier [29]. The H^+ ion beam overlaps with the effusive beam of target gas molecule CO_2 at the center of the collision chamber. The momentum spectrometer is a single field time-of-flight spectrometer combined with a two-dimensional position (x, y) sensitive detector. The ion acceleration region is of length 110 mm followed by a field-free drift region of length 220 mm, satisfying the Wiley-McLaren space focusing condition [30]. The fragment ions are guided toward the detector by a uniform electric field of strength 60 V/cm. The direction of the field is taken to be the $+z$ direction. The ion detector is an 80-mm-diam microchannel plate with a delay-line anode. Ejected electrons are detected by a channeltron mounted on the opposite side, which triggers the start of the ion time-of-flight measurement. Ion time-of-flight (t) and arrival positions (x, y) are recorded in list-mode format. Recorded data are analyzed offline. Raw selection of three-body fragmentation events is by a simple triple ion coincidence condition; further refinement is done by imposing the momentum conservation condition, ensuring that the ionic fragments arise from the dissociation of the same molecular ion [29]. The low ion beam current (10–15 pA), and the low effusive gas pressure (estimated 10^{-4} mbar) and excellent background pressure (2×10^{-7} mbar), keep accidental coincidences low. The t, x, y information is mapped one to one to the momentum components p_z, p_x, p_y of fragments. From this information, the kinetic energy of all ionic fragments is derived. An extraction field of 60 V/cm results in a moderate three-body KER resolution of (≈1.0 eV) and 4π collection for ions with energy <5 eV/q.

III. RESULTS AND DISCUSSION

The observed fragments $O^+ + C^+ + O^+$ can be formed either via a simultaneous breaking of the two bonds (the concerted mechanism), or a stepwise breaking of the two bonds, involving a briefly lived CO^{2+} intermediate (the sequential mechanism). The two mechanisms are expected to result in not only differing angular correlations between the momentum vectors of the three fragments, but also differing KER distributions. Events corresponding to the two mechanisms can be separated using the Dalitz representation [6]. We analyze the Dalitz plots and the KER distributions of the fragments to understand the dynamics of the breakup of CO_2^{3+} and the participation of different excited states, and we examine how a small variation in the energy of the proton projectiles affects these. Comparing our spectra with those for other HCI and electron impact, we identify the contributions from different intermediate states of CO_2^{3+} to the KER spectra for a variety of projectiles.

A. Correlations between fragment momenta

A Dalitz plot permits visualization of the correlated momenta of three fragments in terms of their reduced kinetic energies. The x and y coordinates of a Dalitz plot are given by

$$x = \frac{E_1 - E_3}{3^{1/2} E_T}, \quad y = \frac{E_2}{E_T} - \frac{1}{3}, \tag{1}$$

where E_i ($i = 1, 2, 3$) are the kinetic energies of the three fragments, and E_T is the total kinetic energy release, $E_1 + E_2 + E_3$. For the present case, the subscript i corresponds to $O^+_{(1)}$, C^+, $O^+_{(2)}$, respectively. Figure 1 shows the Dalitz plot for this breakup due to 0.5 a.u. H^+ impact. As detailed in [6], the bottom oval-shaped area represents a concerted breakup in which both bonds of CO_2^{3+} break simultaneously in a linear or bent configuration, while the area appearing as a V-shaped band corresponds to a sequential breakup with an intermediate $O^+ + CO^{2+}$ stage. The Dalitz plot for 0.83 a.u. impact is essentially similar and is not shown.

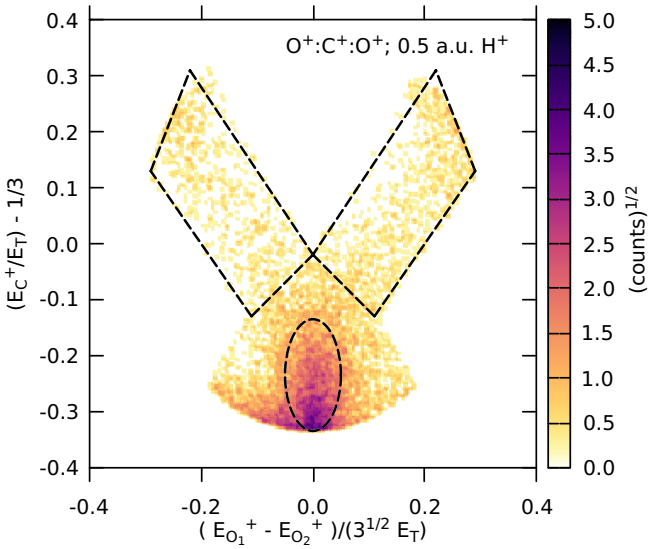

FIG. 1. Dalitz plot for the $O^+ + C^+ + O^+$ breakup under 0.5 a.u. H^+ impact. The ellipse encloses events that are due to concerted breakup, while the quadrilaterals enclose events due to sequential breakup.

Based on these separations, we can obtain the KER distributions corresponding to the sequential and concerted processes leading to the same final fragments. It is known from previous studies that the concerted process results in higher KER values compared to the sequential process. Several previous reports confirm these broad conclusions [6,15,19]. We now turn our attention to the KER distributions for the two breakup mechanisms.

B. Kinetic energy release distributions

The total KER distributions under the impact of H^+ ions at energies of 0.5 and 0.83 a.u. are shown in Fig. 2. The distributions for the constituent sequential and concerted breakups, separated with the aid of the Dalitz plot, are also shown. The total KER distribution lies higher than the sum of the two contributions, since the separation is partial and excludes some events. The total KER distributions for both impact energies have the main peak at 21 eV and another less prominent feature at 28 eV. However, for 0.83 a.u. impact another feature becomes prominent near 15 eV. Since KER distributions for

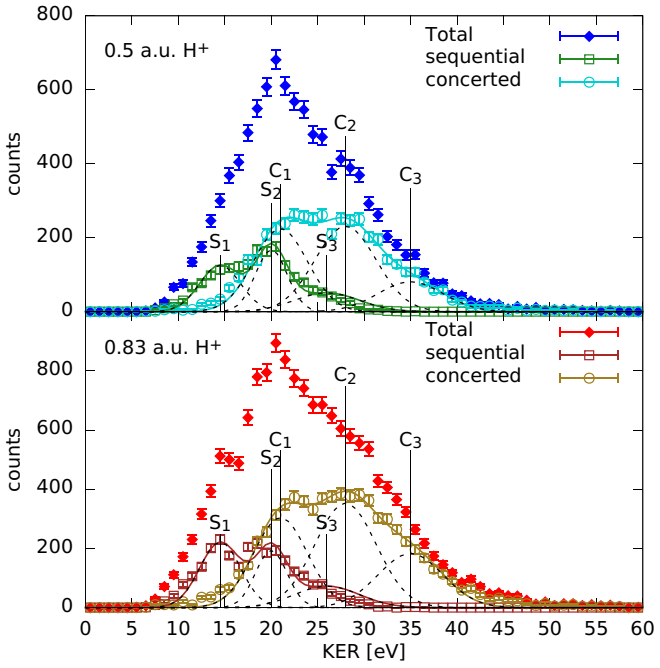

FIG. 2. KER distributions for the $O^+ + C^+ + O^+$ breakup under $v = 0.5$ and 0.83 a.u. H^+ impact. Error bars on the experimental data show statistical errors. The total KER distribution is separated into contributions from sequential and concerted breakups based on the Dalitz plot (events enclosed in the quadrilaterals and the ovals which are overlaid on the Dalitz plot in Fig. 1). The total KER distribution lies higher than the sum of the two contributions, since the separation is approximate and excludes some events. The sequential and concerted breakup data are separately fitted to the sum of three Gaussian functions each. They are identified as S_1, S_2, S_3 and C_1, C_2, C_3, and they have centroids at 14.5, 20, and 26 eV and at 21, 28, and 35 eV, respectively.

both impact velocities arise from the same set of excited states of CO_2^{3+}, we identify local maxima in the spectra for the two impact energies, and we assign the corresponding KER value as a possible peak position for all spectra. This approximation helps us identify features clearly and establish the contrast in the effects at two impact velocities. Three common features of varying intensity can be seen in each of the distributions for sequential and concerted breakup, and these are identified as S_1, S_2, S_3 and C_1, C_2, C_3, respectively. For both types of breakup, two of the features are strong and the third one is weak.

Further analysis is done by fitting the sequential and concerted components separately to the sum of three Gaussian functions. The centroids μ of the Gaussians are 14.5, 20, and 26 eV for the sequential components, and 21, 28, and 35 eV for the concerted components. The centroids are determined by a combination of the location of the features seen in the KER distributions and the most probable values expected from the Franck-Condon (FC) overlap of the CO_2 ground state with the CO_2^{3+} states. The potential energy curve (PEC) of the latter set of states is taken from Wang *et al.* [20]. The width of the Gaussian function used for fitting to the KER distribution cannot be readily determined. It is approximately determined based on the slope of the PEC of the upper state and the width of the FC region, taking care that the width of the function is larger for steeper PECs. The amplitudes of the Gaussian functions are then determined by a least-squares fit to the experimental distribution. It should be noted that the PECs reported by Wang *et al.* are approximate. They have been computed for a linear symmetric geometry and for large intervals of the internuclear separations. Furthermore, the computations are done keeping the core orbitals closed, and only valence orbitals are taken to be active. Hence only limited accuracy is expected in the assignment of the states and the KER values.

Areas under the Gaussian curves thus obtained are listed in Table I for both impact energies. Since the collection efficiency of the spectrometer is less than unity for high-energy fragments, a correction needs to be applied to the high-energy part of the KER distribution. The correction will generally enhance the features at high KER values compared to the low-energy ones. This aspect has been elaborated upon for the case of a two-body breakup [31]. However, for a three-body breakup, which has a combination of sequential and concerted processes, the correction factor is complicated and will also depend on the geometry of the dissociating molecule. No systematic study of this correction appears to have been done so far. Thus, while the areas under the fitted peaks in Table I can be compared for different projectiles in the same experimental conditions, care should be taken in comparing with other reports. We see that for $v = 0.5$ a.u., the states corresponding to features S_1 and S_2 contribute nearly equally in the sequential breakup. On the other hand, for $v = 0.83$ a.u. the S_1 feature at 14.5 eV is enhanced by ≈8% while the S_2 feature at 20 eV is suppressed by a similar amount, indicating that the faster impact results in relatively higher probability of exciting low-lying electronic states $^2\Pi, ^4\Pi$ of CO_2^{3+}, as compared to the slower impact. Faster H^+ impact has also resulted in enhancement of the feature C_3 at 35 eV from a concerted breakup, corresponding to $^8\Pi, ^8\Sigma^+$ states. We also find that the contribution of sequential breakup to total events at both impact energies is ≈18%. This ratio has been reported to be around 20% for Ar^{8+} impact [6,15] and 12% for electron impact [20]. These observations show that a change of projectile considerably influences the relative contributions of different breakup mechanisms.

C. Comparison with other projectiles

To contrast the excitation by protons with that by other projectiles, we compare the total KER distributions from the present investigation and from the literature. Significant differences can be seen (see Fig. 3) between the present data and the data from previous experiments with slow HCIs [6,15] and electron impact [20]. We find that the total KER distributions are well fitted by the sum of multiple Gaussians with the same values of the centroids and widths as in our proton impact data. Based on the fits, the contribution of different features in these reports can be identified. However, since the features S_2, C_1 and S_3, C_2 are very close-lying and cannot be separated in the total KER, these pairs of features are taken together while making the comparison.

In the report by Neumann *et al.* [6] for the $O^+ + C^+ + O^+$ breakup exclusively via capture ionization by 0.31 a.u. Ar^{8+}

TABLE I. Areas under the Gaussian curves fitted to the KER distributions of sequential and concerted breakups under proton impact. KER distributions of the two types of breakups are separately area-normalized to unity. S_1, S_2, S_3 and C_1, C_2, C_3 are the features in KER distributions of sequential and concerted breakups, respectively. The centroids of these features are in fair agreement with the estimates from the computed PECs of Wang *et al.* [20]; the identification of the participating states is also based on the same report. Errors shown are fitting errors.

	Feature, centroid, and probable contributing states					
Projectile	S_1(14.5)	S_2 (20)	S_3 (26)	C_1 (21)	C_2 (28)	C_3 (35)
speed	$(^2\Pi,^4\Pi)$	$(^2\Sigma^+,^4\Sigma^+)$	$(^6\Sigma^+,^6\Pi)$	$(^2\Sigma^+,^4\Sigma^+)$	$(^6\Sigma^+,^6\Pi)$	$(^8\Pi,^8\Sigma^+)$
0.5 a.u.	0.38 ± 0.02	0.39 ± 0.01	0.24 ± 0.04	0.37 ± 0.01	0.43 ± 0.01	0.16 ± 0.01
0.83 a.u.	0.46 ± 0.02	0.31 ± 0.02	0.24 ± 0.04	0.31 ± 0.01	0.41 ± 0.01	0.23 ± 0.01

impact, the total KER distribution is in the range 15–40 eV, and it is found to be composed mainly of contributions from features S_2, C_1 and from S_3, C_2. There is negligible contribution from S_1 and C_3. In contrast, in the report of Khan *et al.* [15] for Ar^{8+} at $v = 1$ a.u., the KER distribution extends from 15 to 50 eV with no contribution from feature S_1, significant contributions from S_2, C_1 and S_3, C_2, and a weaker contribution from C_3. The main difference in the KER distribution of fragments for the two impact velocities of the same projectile is that the KER distribution is broader for the faster projectile and has contributions from higher-lying states of CO_2^{3+}. This is plausible, since at higher projectile velocities close encounters are more probable, leaving the molecular ion in comparatively higher-lying electronically excited states.

The only detailed report for electron-impact triple ionization of CO_2 is for $v = 6.1$ a.u. (500 eV) by Wang *et al.* [20]. There the KER distribution ranges from 10 to 50 eV with contributions of all features with varying intensities. The main difference from the HCI case is the appearance of the feature S_1, which is also seen in the present proton impact data. The appearance of this feature was attributed to the difference in the ionization mechanisms: slow HCI impact predominantly causes multiple electron capture, and it does not populate the lowest states $^2\Pi$ and $^4\Pi$, whereas under electron impact there is a propensity to populate the lowest-lying states. The rest of the features in their data (viz. S_3, C_2, C_3) are comparable in intensity to that for 1 a.u. Ar^{8+} as well as the present proton impact data.

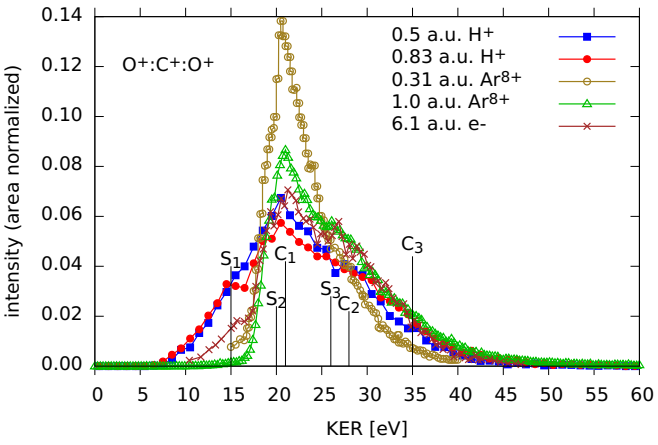

FIG. 3. KER distributions for the $O^+ + C^+ + O^+$ breakup for the present $v = 0.5$ and 0.83 a.u. H^+ impact experiment (filled symbols) compared with the results from the literature for HCI impact at different velocities (open symbols [6,15]) and electron impact at $v = 6.1$ a.u. (crosses [20]). The prominent low-energy feature, S_1, is common to electron and proton impact, but not seen at all in HCI impact. Feature C_3 is seen for all projectiles except 0.31 a.u. Ar^{8+} [6], for which the dominant process is capture ionization. Each distribution is separately area-normalized to its total counts.

We see in Fig. 3 that the KER distribution for slow H^+ ion impact shows all of the features of electron impact and also an overall range comparable to that for slow HCI impact considered here. The noteworthy point is that under electron impact, electron capture is impossible and multiple ionization can occur only by direct ionization. So the S_1 feature cannot arise from electron capture. Scully *et al.* [32] have shown that the contribution of inner shell ionization is significant at these electron energies, along with outer shell ionization. It should be noted that proton impact with $v < 1$ results in ionization only from the outer shell of the target [33]. However, inner shell ionization will, by and large, lead to high-lying states of CO_2^{3+}, and thus higher KER values. Consequently, it will not contribute to the S_1 feature. Slow protons cause multiple ionization via direct ionization or single capture processes, whereas slow HCIs cause multiple ionization mainly through multiple capture of electrons from a target molecule with negligible direct ionization, generally resulting in a narrower KER range [6,34,35]. In particular, as seen in Fig. 3, low-lying electronic states of CO_2^{3+}, corresponding to the S_1 feature, which are accessed under proton impact, are not accessed in ionization via electron capture by a multielectron projectile.

Putting together our proton impact results and the results of HCI and electron impact, it can be concluded that the S_1 feature must arise due to direct ionization of outer shells, which result in low-lying CO_2^{3+} excited $^2\Pi,^4\Pi$ states. The enhanced S_1 feature under 0.83 a.u. H^+ impact (as opposed to 0.5 a.u. impact) is likely to be due to the increased probability of direct ionization. In this proton energy range, the cross-sections for direct and capture ionization are comparable and show opposite tendencies with increasing impact energy [35,36]. Further enhancement in the S_1 feature can be anticipated with increasing proton energy until inner shell ionization contributes significantly.

IV. CONCLUSION

Triple ionization of CO_2, populating a wide range of transient states, can be achieved by even the simplest of ions—the proton—in the velocity range $v < 1$ a.u. In spite of it being a structureless projectile, a small variation in the impact

velocity of the proton affects the breakup dynamics in this regime. This is because of the changes in the relative contribution of different ionization mechanisms with a change in impact velocity.

A particularly noteworthy feature in the KER distribution for triple fragmentation of CO_2^{3+} is the one around 15 eV, which has been reported for electron impact, but not for HCI impact. The feature is found to be stronger for 0.83 a.u. than for 0.5 a.u. proton impact in the present study. It is argued that this feature results from dissociation via low-lying $^2\Pi,^4\Pi$ electronic states of CO_2^{3+}. In an energy range where the cross-sections for electron capture and direct ionization compete with each other, a small variation in impact energy results in enhanced access to low-lying electronic states of CO_2^{3+} via direct ionization of the outer shells of CO_2. Ionization by protons may involve capture, which is impossible with electron projectiles, but both can induce direct ionization. Especially with fast ($v \gg 1$ a.u.) electrons, inner shell ionization will be significant, while slow ($v < 1$ a.u.) protons will mainly induce direct ionization or capture from outer shells. Despite these differences, we find that the KER distribution for the triple fragmentation with slow protons shows nearly all the features seen with fast electrons.

Limitations of our experimental setup do not currently permit separation of capture and direct ionization mechanisms, which may be addressed by more involved experimental strategies comprising electron spectroscopy and postcollision projectile charge state analysis. Further, it would be interesting to study the breakup dynamics and the changes in the breakup patterns at higher proton impact velocities ($v > 1$), since in that regime a competition between processes such as capture and direct ionization from outer and inner shells of the target is expected. Also needed are accurate potential energy curves of CO_2^{3+}, including asymmetric configurations, for a proper comparison with experimental KER values and exact identification of the transient states responsible for the observed breakup patterns.

ACKNOWLEDGMENTS

The authors thank the Dept. of Science and Technology, Science and Engineering Research Board (India) for generous funding via grant No. 30116294, which enabled the setting up of the EBIS/A ion source used for this work. They would also like to acknowledge technical help from Dreebit GmbH and assistance from the technical staff at IISER Pune in setting up and running the machine. We thank the authors of previous reports [6,15,20] for sharing their KER data with us for the purpose of comparison.

[1] A. Brahme, Int. J. Radiat. Oncol. Biol. Phys. **58**, 603 (2004).
[2] H. Chang, W. Oehrl, P. Elsner, and J. J. Thiele, Free Rad. Res. **37**, 655 (2003).
[3] D. T. Hall, D. F. Strobel, P. D. Feldman, M. A. McGrath, and H. A. Weaver, Nature (London) **373**, 677 (1995).
[4] H.-K. Kim, J. Titze, M. Schöffler, F. Trinter, M. Waitz, J. Voigtsberger, H. Sann, M. Meckel, C. Stuck, U. Lenz, M. Odenweller, N. Neumann, S. Schössler, K. Ullmann-Pfleger, B. Ulrich, R. C. Fraga, N. Petridis, D. Metz, A. Jung, R. Grisenti *et al.*, Proc. Natl. Acad. Sci. (USA) **108**, 11821 (2011).
[5] J. D. Savee, V. A. Mozhayskiy, J. E. Mann, A. I. Krylov, and R. E. Continetti, Science **321**, 826 (2008).
[6] N. Neumann, D. Hant, L. P. H. Schmidt, J. Titze, T. Jahnke, A. Czasch, M. S. Schöffler, K. Kreidi, O. Jagutzki, H. Schmidt-Böcking, and R. Dörner, Phys. Rev. Lett. **104**, 103201 (2010).
[7] R. Dörner, V. Mergel, O. Jagutzki, L. Spielberger, J. Ullrich, R. Moshammer, and H. Schmidt-Böcking, Phys. Rep. **330**, 95 (2000).
[8] J. Ullrich, R. Moshammer, A. Dorn, R. Dörner, L. P. H. Schmidt, and H. Schmidt-Böcking, Rep. Prog. Phys. **66**, 1463 (2003).
[9] Y. Wang, X. Shi, J. Zhou, S. Xu, D. Guo, S. Yan, X. Zhu, and X. Ma, Phys. Rev. A **101**, 042706 (2020).
[10] R. Guillemin, P. Decleva, M. Stener, C. Bomme, T. Marin, L. Journel, T. Marchenko, R. K. Kushawaha, K. Jänkälä, N. Trcera, K. P. Bowen, D. W. Lindle, M. N. Piancastelli, and M. Simon, Nat. Commun. **6**, 6166 (2015).
[11] B. Wales, R. Karimi, E. Bisson, S. Beaulieu, M. Giguère, T. Motojima, R. Anderson, J. Matsumoto, J.-C. Kieffer, F. Légaré, H. Shiromaru, and J. Sanderson, Phys. Scr. **T156**, 014068 (2013).
[12] A. Khan and D. Misra, J. Phys. B **49**, 055201 (2016).
[13] Z. Shen, E. Wang, M. Gong, X. Shan, and X. Chen, J. Chem. Phys. **145**, 234303 (2016).
[14] S. Srivastav, A. Sen, D. Sharma, and B. Bapat, Phys. Rev. A **103**, 032821 (2021).
[15] A. Khan, L. C. Tribedi, and D. Misra, Phys. Rev. A **92**, 030701(R) (2015).
[16] B. Siegmann, U. Werner, H. O. Lutz, and R. Mann, J. Phys. B **35**, 3755 (2002).
[17] M. R. Jana, P. N. Ghosh, B. Bapat, R. K. Kushawaha, K. Saha, I. A. Prajapati, and C. P. Safvan, Phys. Rev. A **84**, 062715 (2011).
[18] L. Adoui, T. Muranaka, M. Tarisien, S. Legendre, G. Laurent, A. Cassimi, J.-Y. Chesnel, X. Fléchard, F. Frémont, B. Gervais, E. Giglio, and D. Hennecart, Nucl. Instrum. Methods Phys. Res., Sect. B **245**, 94 (2006), swift Heavy Ions in Matter.
[19] S. Yan, X. L. Zhu, P. Zhang, X. Ma, W. T. Feng, Y. Gao, S. Xu, Q. S. Zhao, S. F. Zhang, D. L. Guo, D. M. Zhao, R. T. Zhang, Z. K. Huang, H. B. Wang, and X. J. Zhang, Phys. Rev. A **94**, 032708 (2016).
[20] E. Wang, X. Shan, Z. Shen, M. Gong, Y. Tang, Y. Pan, K.-C. Lau, and X. Chen, Phys. Rev. A **91**, 052711 (2015).
[21] P. Bhatt, R. Singh, N. Yadav, and R. Shanker, Phys. Rev. A **85**, 042707 (2012).
[22] R. K. Singh, G. S. Lodha, V. Sharma, I. A. Prajapati, K. P. Subramanian, and B. Bapat, Phys. Rev. A **74**, 022708 (2006).
[23] R. K. Kushawaha, S. S. Kumar, I. A. Prajapati, K. P. Subramanian, and B. Bapat, J. Phys. B **42**, 105201 (2009).
[24] W. A. Bryan, J. H. Sanderson, A. El-Zein, W. R. Newell, P. F. Taday, and A. J. Langley, J. Phys. B **33**, 745 (2000).

[25] J. P. Brichta, S. J. Walker, R. Helsten, and J. H. Sanderson, J. Phys. B **40**, 117 (2006).
[26] I. Bocharova, R. Karimi, E. F. Penka, J.-P. Brichta, P. Lassonde, X. Fu, J.-C. Kieffer, A. D. Bandrauk, I. Litvinyuk, J. Sanderson, and F. Légaré, Phys. Rev. Lett. **107**, 063201 (2011).
[27] C. Wu, C. Wu, D. Song, H. Su, Y. Yang, Z. Wu, X. Liu, H. Liu, M. Li, Y. Deng, Y. Liu, L.-Y. Peng, H. Jiang, and Q. Gong, Phys. Rev. Lett. **110**, 103601 (2013).
[28] B. Bapat, D. Sharma, and S. Srivastav, J. Phys.: Conf. Ser. **1412**, 152070 (2020).
[29] V. Sharma and B. Bapat, European Phys. J. D **37**, 223 (2006).
[30] W. C. Wiley and I. H. McLaren, Rev. Sci. Instrum. **26**, 1150 (1955).
[31] A. Pandey and B. Bapat, Int. J. Mass Spectrom. **361**, 23 (2014).
[32] S. W. J. Scully, J. A. Wyer, V. Senthil, M. B. Shah, and E. C. Montenegro, Phys. Rev. A **73**, 040701(R) (2006).
[33] V. V. Afrosimov, A. A. Basalaev, G. N. Ogurtsov, and M. N. Panov, Tech. Phys. **59**, 642 (2014).
[34] H. O. Folkerts, R. Hoekstra, and R. Morgenstern, Phys. Rev. Lett. **77**, 3339 (1996).
[35] E. Wells, V. Krishnamurthi, K. D. Carnes, N. G. Johnson, H. D. Baxter, D. Moore, K. M. Bloom, B. M. Barnes, H. Tawara, and I. Ben-Itzhak, Phys. Rev. A **72**, 022726 (2005).
[36] F. Gobet, S. Eden, B. Coupier, J. Tabet, B. Farizon, M. Farizon, M. J. Gaillard, M. Carré, S. Ouaskit, T. D. Märk, and P. Scheier, Phys. Rev. A **70**, 062716 (2004).